Bioorganic & Medicinal Chemistry Letters 19 (2009) 1451–1456

Contents lists available at ScienceDirect

Bioorganic & Medicinal Chemistry Letters

journal homepage: www.elsevier.com/locate/bmcl

Design, synthesis and structure–activity relationships of azole acids as novel, potent dual PPAR α/γ agonists

Hao Zhang [a], Denis E. Ryono [a], Pratik Devasthale [a], Wei Wang [a], Kevin O'Malley [c], Dennis Farrelly [b], Liqun Gu [b], Thomas Harrity [b], Michael Cap [b], Cuixia Chu [b], Kenneth Locke [c], Litao Zhang [c], Jonathan Lippy [c], Lori Kunselman [b], Nathan Morgan [b], Neil Flynn [b], Lisa Moore [b], Vinayak Hosagrahara [d], Lisa Zhang [d], Pathanjali Kadiyala [e], Carrie Xu [e], Arthur M. Doweyko [g], Aneka Bell [h], Chiehying Chang [f], Jodi Muckelbauer [f], Robert Zahler [a], Narayanan Hariharan [b], Peter T. W. Cheng [a,*]

[a] Metabolic Diseases Chemistry, Bristol-Myers Squibb Research and Development, Princeton, NJ 08543-5400, USA
[b] Metabolic Diseases Biology, Bristol-Myers Squibb Research and Development, Princeton, NJ 08543-5400, USA
[c] Lead Evaluation, Bristol-Myers Squibb Research and Development, Princeton, NJ 08543-5400, USA
[d] Metabolism and Pharmacokinetics, Bristol-Myers Squibb Research and Development, Princeton, NJ 08543-5400, USA
[e] Bio-Analytical Research, Bristol-Myers Squibb Research and Development, Princeton, NJ 08543-5400, USA
[f] Macromolecular Crystallography, Bristol-Myers Squibb Research and Development, Princeton, NJ 08543-4000, USA
[g] Computer-Assisted Drug Design, Bristol-Myers Squibb Research and Development, Princeton, NJ 08543-4000, USA
[h] Gene Expression and Protein Biochemistry, Bristol-Myers Squibb Research and Development, Princeton, NJ 08543-4000, USA

ARTICLE INFO

Article history:
Received 10 November 2008
Revised 8 January 2009
Accepted 12 January 2009
Available online 15 January 2009

Keywords:
Dual PPAR α/γ agonists
Azole
Pyrrole
Pyrazole
Triazole
Conformational constraint

ABSTRACT

The design, synthesis and structure–activity relationships of a novel series of *N*-phenyl-substituted pyrrole, 1,2-pyrazole and 1,2,3-triazole acid analogs as PPAR ligands are outlined. The triazole acid analogs 3f and 4f were identified as potent dual PPARα/γ agonists both in binding and functional assays in vitro. The 3-oxybenzyl triazole acetic acid analog 3f showed excellent glucose and triglyceride lowering in diabetic *db/db* mice.

Peroxisome proliferator-activated receptors (PPARs) are a group of nuclear hormone receptors which function as transcription factors in the regulation of genes involved in glucose and lipid fatty acid metabolism and vessel wall function.[1] Three PPAR subtypes have been identified: PPARα, γ and δ. PPARα is predominantly expressed in catabolically active tissues such as liver, heart, kidney, and muscle. It is involved in the uptake and oxidation of fatty acids as well as in lipoprotein metabolism.[2] The clinically used PPARα agonists are the fibrate class of drugs (including fenofibrate[3] and gemfibrozil[4]), which elevate HDL cholesterol levels and lower triglyceride and LDL cholesterol levels. PPARγ is mainly expressed in adipose tissue and regulates insulin sensitivity, glucose and fatty acid utilization as well as adipocyte differentiation. The clinically used PPARγ agonists comprise the thiazolidinedione (TZD) class of anti-diabetic drugs such as rosiglitazone[5] and pioglitazone.[6] It has been hypothesized that the combination of PPARγ and PPARα agonist activities in a single compound would result in synergistic improvements in insulin sensitivity and normalization of glucose metabolism as well as amelioration of the dyslipidemia associated with type 2 diabetes.

We have previously reported on the discovery and exploration of the SAR of the novel oxybenzylglycine series of dual PPARα/γ agonists, which culminated in the discovery of the clinical candidate Muraglitazar **5**.[7a,7b] Compound **5** (Fig. 1) shows potent functional activity in vitro at both human PPARα and PPARγ and excellent efficacy in animal models of type 2 diabetes and the associated dyslipidemia.[7c–e] As part of our ongoing efforts to discover additional novel, potent, highly efficacious and safe dual PPARα/γ agonists with differentiated profiles from muraglitazar, we decided to further explore the SAR of the oxybenzylglycine series by examining the effects of constraining the carbamate N-acid moiety. One of the possible modes of constraint is shown in Figure 1, where the carbamate oxygen is cyclized onto the glycine α-carbon to form a ring. This could be effected through a structure such as an azole, which could be envisioned to be various regioisomers of pyrroles

* Corresponding author. Tel.: +1 609 818 4952; fax: +1 609 818 3460.
E-mail address: peter.t.cheng@bms.com (P.T.W. Cheng).

0960-894X/$ - see front matter © 2009 Elsevier Ltd. All rights reserved.
doi:10.1016/j.bmcl.2009.01.030

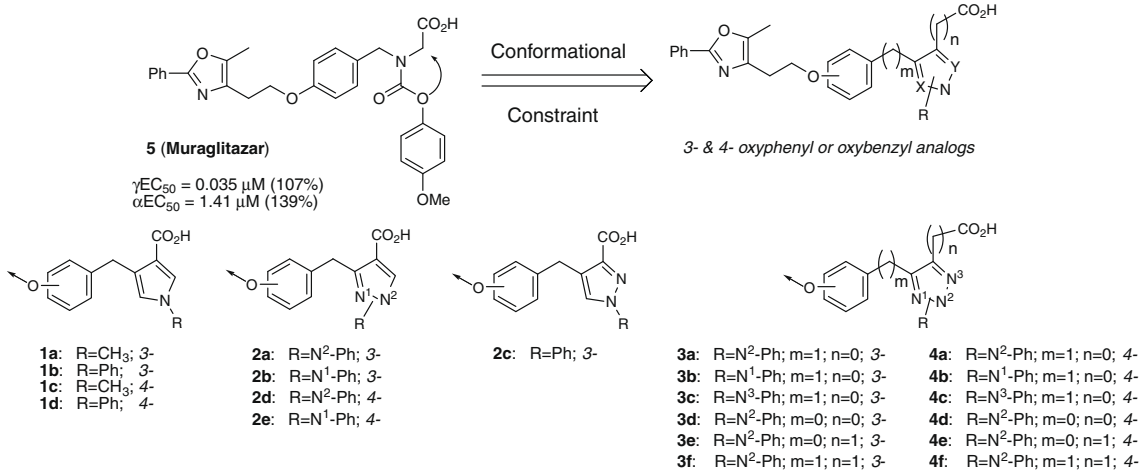

Figure 1. Design of azole acid analogs from oxybenzylglycines.

1a–**1d**, pyrazoles **2a**–**2e**, and triazoles **3a**–**3f** and **4a**–**4f**. We report here a systematic SAR study of this azole acid series, which resulted in the discovery of analogs with distinct PPARα and PPARγ functional activities, of which a number proved to be potent dual PPARα and PPARγ agonists in binding and functional assays in vitro.

An exemplary route to N-substituted pyrrole-3-carboxylic acids **1a**–**1d** is shown in Scheme 1. Wittig reaction of aldehyde **6**[7b] gave the α, β-unsaturated ester **7**, which was reacted with tosylmethyl isocyanide to provide the pyrrole ester **8**.[8] Pyrrole **8** underwent a Cu(I)-mediated coupling reaction[9] with an appropriate arylboronic acid to provide the corresponding *N*-aryl pyrrole ester, which was subsequently deprotected to furnish the N-substituted pyrrole acids **1a**–**1d**.

The synthesis of 5-(3-oxybenzyl)pyrazole-4-carboxylic acid **2a** and 5-(4-oxybenzyl)pyrazole-4-carboxylic acid **2d** is described in Scheme 2. Methyl cyanoacetate was alkylated with benzyl chloride **9**, followed by ester hydrolysis to provide cyanoacetic acid **10**.[10] Treatment of **10** with a phenyl diazonium salt (generated in situ) provided the corresponding cyano-hydrazone **11**. Reaction of **11** with methyl acrylate under basic conditions[11] generated the key pyrazole ester intermediate **12**. Finally, a three-step sequence involving: (1) demethylation of anisole **12**, (2) alkylation of phenol with 2-[5-methyl-2-phenyloxazol-4-yl] ethyl mesylate and (3) deprotection of the carboxylic acid, furnished **2a** and **2d**.

A synthesis of the regioisomeric carboxypyrazole **2c** is shown in Scheme 3. Treatment of aldehyde **13** with ethynylmagnesium bromide furnished the acetylenic alcohol adduct **14**. Thermolysis of **14** with ketene dimer[12] provided the corresponding acetoacetate ester, which was chlorinated to provide the α-chloro-β-ketoester **15**. Heating of **15** with a phenyl diazonium salt (generated in situ) furnished the chlorohydrazone **16**.[13] Base-mediated thermal intramolecular cycloaddition of **16** then furnished the pyrazole-lactone **17**. Concomitant ring-opening/deoxygenation of **17** could be achieved with TMSI[14] to furnish the pyrazole ester **18**. The same three-step sequence: (a) removal of the phenolic protect-

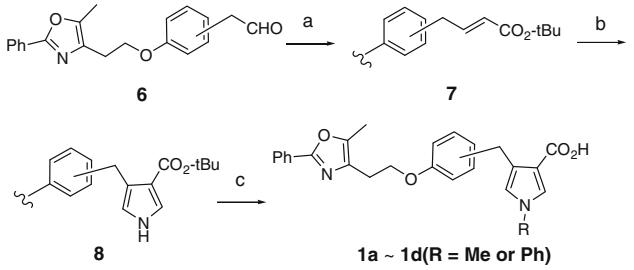

Scheme 1. The synthesis of **1a**–**1d**: (a) Ph_3PCHCO_2tBu, toluene, reflux, 80%; (b) 4-Me-C_6H_4-SO_2CH_2NC, NaH, DMSO, 70%; (c) i—$RB(OH)_2$, Cu(I) salt, base or RX, base; ii—TFA 50-70%.

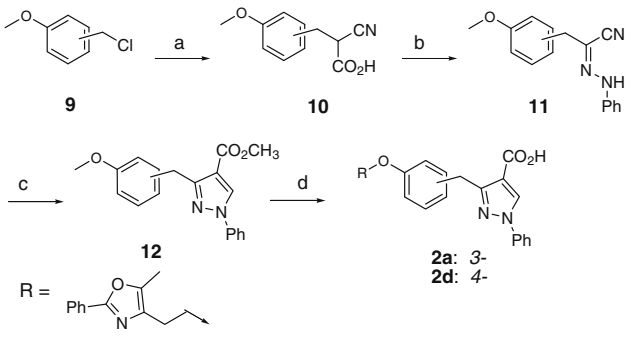

Scheme 2. The synthesis of **2a** and **2d**: (a) i—$NCCH_2CO_2CH_3$, CH_3ONa, CH_3OH, 52%; ii—NaOH, 95%; (b) $PhN_2^+Cl^-$, 11%; (c) i—methyl acrylate, NaH, rt, $(C_2H_5)_3N$, 33%; (d) i—BBr_3, CH_3OH, 25–30%; ii—2-(5-methyl-2-phenyloxazol-4-yl)ethyl methanesulfonate, K_2CO_3, CH_3CN, 90 °C, 12 h, 90%; iii—NaOH, THF, H_2O, 90%.

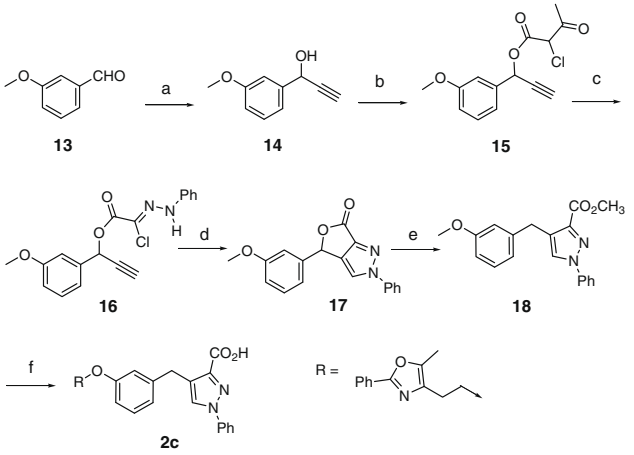

Scheme 3. The synthesis of **2c**: (a) HC≡CMgBr, 79%; (b) i—ketene dimer, Et_3N; ii—SO_2Cl_2, 40%; (c) $PhN_2^+Cl^-$, 94%; (d) Et3N, toluene, reflux, 69%; (e) TMSCI, NaI, CH_3CN, reflux, 81%; (f) i—BBr_3, CH_3OH; ii—2-(5-methyl-2-phenyl-oxazol-4-yl)ethyl methanesulfonate, K_2CO_3, CH_3CN, 90 °C, 12 h; iii—NaOH, 70%.

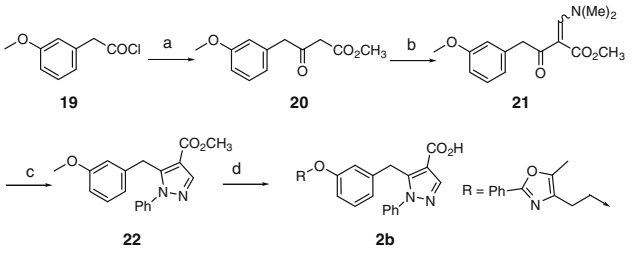

Scheme 4. The synthesis of **2b**: (a) i—Meldrum's acid, pyridine, 0 °C; ii—CH_3OH, reflux, 80%; (b) $(CH_3)_2NCH(OCH_3)_2$, 0 °C, 32%; (c) $PhNHNH_2$, 100 °C, 77%; (d) i—BBr3/MeOH; ii—2-(5-methyl-2-phenyloxazol-4-yl)ethyl methanesulfonate, K_2CO_3, CH_3CN, 90 °C, 12 h; iii—NaOH, 75%.

ing group of **18**, (b) alkylation of the resulting phenol with 2-(5-methyl-2-phenyloxazol-4-yl)ethyl mesylate and (c) ester hydrolysis, furnished the N-substituted pyrazole-acid **2c**.

Scheme 4 illustrates the synthesis of the regioisomeric 1,3-alkoxybenzyl 1-phenyl-3-carboxy-pyrazole analog **2b**. Reaction of phenylacetyl chloride **19** with Meldrum's acid under basic conditions, followed by methanolysis, furnished the β-ketoester **20**. Treatment of **20** with dimethylformamide dimethyl acetal[15] gave the α-enamino-β-keto-ester **21**. The reaction of **21** with phenylhydrazine followed by intramolecular cyclization, provided the *N*-phenyl-pyrazole ester **22**. The same three-step sequence: (a) demethylation of anisole **22**, (b) alkylation of phenol with 2-(5-methyl-2-phenyloxazol-4-yl) ethyl mesylate and (c) deprotection of the carboxylic acid, furnished the 5-benzyl-1-phenyl-1H-pyrazole-4-carboxylic acid **2b**.

The synthesis of the 5-oxybenzyl-2-phenyl-2H-1,2,3-triazole-4-carboxylic acids **3a, 3d** and **4a, 4d** is described in Scheme 5; only the desired "N-2"-phenyl regioisomer should be obtainable by this route. Reaction of a suitably protected oxybenzoic or oxyphenylacetic acid chloride **23** with Meldrum's acid in the presence of base provided the corresponding crude acylation product which was immediately reacted with aniline to give the β-keto anilide **24**.[16] The keto-amide **24** was reacted with nitrous acid (generated in situ from acid/sodium nitrite), then with acid to furnish the corresponding α-oxime β-keto amide.[17] The α-oxime-ketone was then condensed with phenylhydrazine to provide the corresponding β-hydrazone-α-oxime-ketone **25**. $CuSO_4$-mediated cyclization of

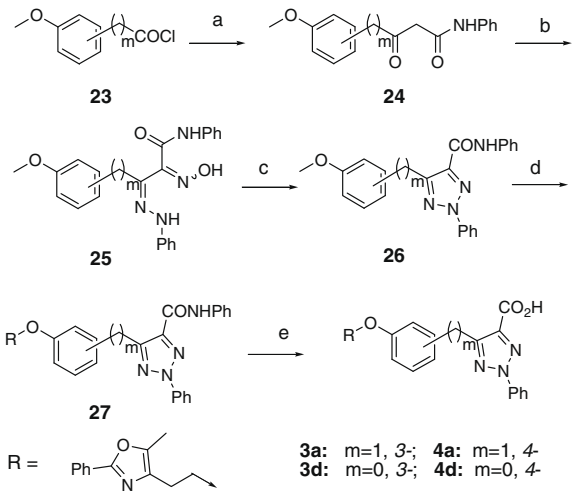

Scheme 5. The synthesis of **3a**, **3d, 4a** and **4d**: (a) i—Meldrum's acid, pyridine, 0 °C, 2 h, rt, 2 h; ii—aniline, reflux, 3 h, 80%; (b) i—$NaNO_2$, H_2SO_4, 0 °C, 30 min; ii—$PhNHNH_2$, EtOH, reflux, 2 h, 56%; (c) i—$CuSO_4$, pyridine; ii—Zn, HCl, 1 h, 89%; (d) i—BBr_3; ii—2-(5-methyl-2-phenyloxazol-4-yl)ethyl methanesulfonate, K_2CO_3, MeCN, 90 °C, 12 h; iii—KOH, EtOH, 90 °C, 24 h, 70%.

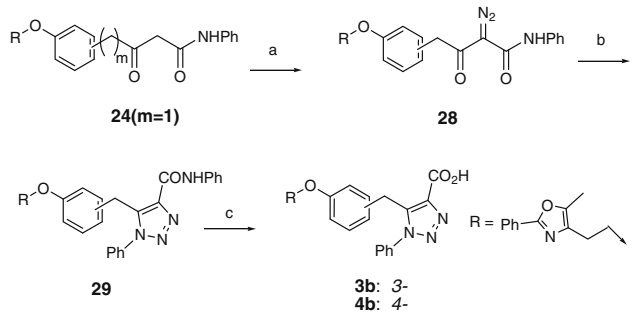

Scheme 6. The synthesis of **3b** and **4b**: (a) TsN_3, Et_3N, rt, 2.5 h, 77%; (b) $PhNH_2$, $TiCl_4$, 80 °C, 2 h, 90%; (c) i—BBr_3, 85–90%; ii—2-(5-methyl-2-phenyloxazol-4-yl) ethylmethanesulfonate, K_2CO_3, CH_3CN, 90 °C, 12 h, 90%; iii—KOH, EtOH, 90 °C, 24 h, 30–70%.

oxime-hydrazone **25** followed immediately by reduction (Zn/HCl) furnished the desired 1,2,3-triazole **26**.[18] The similar three-step sequence: a) demethylation of **26,** (b) alkylation of phenol with 2-(5-methyl-2-phenyloxazol-4-yl) ethyl mesylate and (c) deprotection of the triazole-amide **27** furnished 5-oxybenzyl-2-phenyl-2H-1,2,3-triazole-4-carboxylic acids **3a**, **3d**, **4a**, and **4d**.[19]

The synthesis of the "N-1" aryl triazole isomer **3b** and **4b** is shown in Scheme 6. Treatment of β-keto anilide **24** with *p*-toluenesulfonyl azide[20] furnished the corresponding β-keto α-diazo-anilide **28**. Lewis acid-mediated reaction of **28** with aniline provided the corresponding 5-alkoxybenzyl-1-phenyl-1H-1,2,3-triazole-4-carboxylic acid **29**.[21] A three-step sequence: (a) BBr_3-mediated demethylation of **29**; (b) alkylation of the resultant phenol-triazole with 2-(5-methyl-2-phenyloxazol-4-yl)ethyl mesylate and, (c) basic hydrolysis of the anilide, provided the 5-oxybenzyl-1-phenyl-1H-1,2,3-triazole-4-carboxylic acid **3b** or **4b**.

The synthesis of the 1-phenyl-1H-1,2,3-triazole-5-carboxylic acid **3c** and **4c** was accomplished using the route described in Scheme 7. Ethyl propiolate was added to aldehyde **30** under basic conditions[22] to furnish the corresponding acetylenic alcohol adduct **31**. Deoxygenation of alcohol **31** (Et_3SiH/BF_3-OEt_2)[23] provided the acetylenic ester **32**. Dipolar cycloaddition of the acetylenic ester **32** with phenyl azide under thermal conditions[24] furnished, after deprotection of the carboxylic acid, a ~1:2 mixture of the desired 1-phenyl-1H-1,2,3-triazole-5-carboxylic acids **3c** and **4c** as well as the regioisomeric 1-phenyl-1H-1,2,3-triazole-4-carboxylic acid **3b** and **4b**. The regioisomers, **3c**/**3b** and **4c**/**4b**, were separated by reverse phase preparative HPLC.

The homologated "N-2"-triazole acetic acids **3f** and **4f** were synthesized as shown in Scheme 8. The 4-carboxy-2-phenyl-2H-1,2,3-triazole **3a** or **4a** was reacted with oxalyl chloride. The resultant acid chloride was converted to the homologated methyl ester of

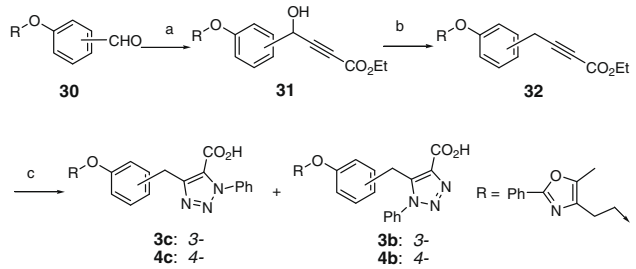

Scheme 7. The synthesis of regioisomeric 1-Ph-substituted-5-carboxy triazoles **3c**/**4c** and 1-Ph-substituted-4-carboxy triazoles **3b**/**4b**: (a) ethyl propiolate, nBuLi/THF, −78 °C, 1 h; (b) $(C_2H_5)_3SiH/BF_3$-Et_2O, 0 °C–rt, 2 h, 50% from **30**; (c) i—PhN_3, 130 °C, 18 h; ii—1 M LiOH/THF, rt, 18 h, 13% for **3c** and **4c**, 26% for **3b** and **4b**.

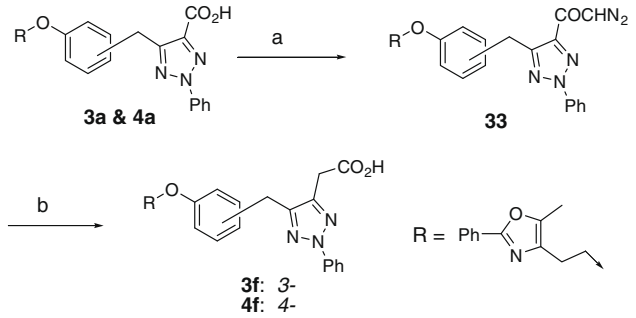

Scheme 8. The synthesis of homologated **3f** and **4f**: (a) i—$(COCl)_2$; ii—CH_2N_2, rt, 2 h, 67%; (b) i—$PhCO_2Ag$, Et_3N, rt, 1 h; ii—1 M LiOH/THF, rt, 18 h, 40%.

3f or **4f** via a silver-mediated Wolff rearrangement of the corresponding α-diazo-ketone **33**.[25]

The PPARα and PPARγ in vitro activities (binding affinity[26] and transactivation activity[27]) of the different series of azole acid analogs are shown in Tables 1–4. From the initial SAR with pyrrole acid analogs **1a**–**1d** (Table 1), we were able to determine that in both the 3- and 4-oxybenzyl series, pyrrole showed some promise as a bioisostere for the carbamate moiety of muraglitazar **5**. Analogs with an *N*-phenyl substituent (**1b** and **1d**) were more potent agonists at PPARγ than the corresponding analogs (**1a** and **1c**) containing an *N*-methyl group. In addition, among these pyrrole-acid analogs, the 3-oxybenzyl substituted pyrrole analog **1b**, which is a relatively selective PPARγ agonist (with only partial activity at PPARα), shows more potent PPARγ activity than the corresponding 4-oxybenzyl analog **1d**.

In the pyrazole series, the regiochemistry of the *N*-phenyl substituent clearly plays an important role in the functional activity. A phenyl group at N^2 appears to be optimal for PPAR activity, as analogs **2a, 2c** and **2d** are more potent PPARγ agonists than the corresponding N^1-aryl substituted pyrazole analogs (e.g., **2b** and **2e**). It

Table 1
In vitro PPAR α and γ activities of pyrrole-acid analogs

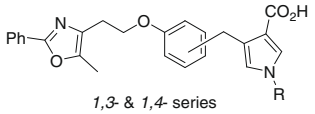

Compound	Oxybenzyl substitution	R	γIC$_{50}$ (μM)	γEC$_{50}$ (μM) IA (%)	αIC$_{50}$ (μM)	αEC$_{50}$ (μM) IA (%)
1a	3-	–CH_3	1.67	2.37 (72%)	5.92	1.47 (26%)
1b	3-	–Ph	0.16	0.55 (82%)	0.09	0.12 (18%)
1c	4-	–CH_3	3.82	1.57 (84%)	>10	>15
1d	4-	–Ph	0.89	4.20 (72%)	0.89	0.66 (13%)

Table 2
In vitro PPAR α and γ activities of pyrazole-acid analogs

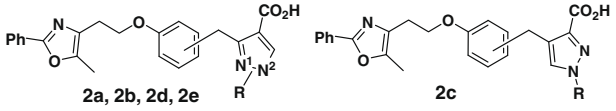

Compound	Oxybenzyl substitution	R	γIC$_{50}$ (μM)	γEC$_{50}$ IA (%) (μM)	αIC$_{50}$ (μM)	αEC$_{50}$ (μM)A (%)
2a	3-	N^2-Ph	0.14	0.023 (76%)	0.07	0.011 (26%)
2b	3-	N^1-Ph	4.74	0.437 (19%)	>25	0.648 (17%)
2c	3-	N-Ph	0.07	0.156 (65%)	0.14	0.311 (24%)
2d	4-	N^2-Ph	2.16	0.752 (90%)	2.17	0.126 (21%)
2e	4-	N^1-Ph	1.67	0.490 (39%)	>25	>25

Table 3
In vitro PPAR α and γ activities of 3- and 4-oxybenzyl triazole acid analogs

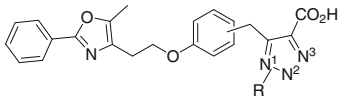

Compound	Oxybenzyl substitution	R	γIC$_{50}$ (μM)	γEC$_{50}$ (μM) IA (%)	αIC$_{50}$ (μM)	αEC$_{50}$ (μM) IA (%)
3[a]	3-	N^2-Ph	0.069	3.79 (70%)	0.069	1.90 (30%)
3b	3-	N^1-Ph	0.75	7.90 (19%)	>25	>15
3c	3-	N^3-Ph	1.48	9.27 (49%)	7.29	>15
4a	4-	N^2-Ph	0.712	9.27 (87%)	2.77	6.15 (52%)
4b	4-	N^1-Ph	10	13.6 (21%)	>25	>15
4c	4-	N^3-Ph	0.88	5.80 (21%)	>7.5	>15

should be noted that all five analogs in these pyrazole-acid series show only partial functional activity at PPARα (in spite of good binding affinity at PPARα for **2a** and **2c**).

The next azole to be explored as a carbamate bioisostere was the 1,2,3-triazole. We systematically examined the effect of all three possible (N^1, N^2 and N^3) regioisomeric phenyl-substituted triazole acids in the context of both the 3- and 4-oxybenzyl series. As in the pyrrole and pyrazole series, the different *N*-phenyl substitution patterns on the triazole ring had a major effect on the PPARα and PPARγ agonist activity of these analogs. In both the 3- and 4-oxybenzyl series, for instance, analogs with N^1 or N^3-phenyl substituents (e.g., **3b**, **3c**, **4b** and **4c**; Table 3), did not show any PPARα agonist activity. Analogs **3a** and **4a**, with an N^2-phenyl group, display relatively more balanced and potent dual PPARα and PPARγ agonist activities. Overall, however, these series of triazole acids displayed relatively poor PPARα/γ functional activities.

Based on the results of this initial SAR survey of the oxybenzyl triazole acids (**3a–c**, **4a–c**, $m = 1$; $n = 0$; Table 3), we then systematically examined the effects of inserting a methylene linker between the oxybenzyl group, the triazole and the acid. The results of this study are shown in Table 4 (using the optimized N^2-phenyl substituent). The relatively constrained 3-oxyphenyl triazole acid **3d** ($m = n = 0$) displayed weak agonist activities at PPARα and PPARγ. Insertion of a methylene linker from the oxyphenyl group to the triazole (i.e., oxybenzyl vs oxyphenyl; **3a** vs **3d**) resulted in a ~10-fold improvement in the binding affinities to PPARα and PPARγ, but surprisingly there was no corresponding improvement in functional activity. Insertion of a methylene between the triazole and the acid in the oxyphenyl series (**3e** vs **3d**, n = 0 vs 1) resulted in not only improved binding affinity (20-fold at PPARγ and 6-fold at PPARα), but also more potent functional activity at both receptors (4-fold at PPARγ and 10-fold at PPAR. Moreover, when the triazole acetic acid is combined with the oxybenzyl moiety (**3f**; $m = 1$ and $n = 1$), this additional structural adjustment resulted in >100-fold increases in both the binding affinity and functional activities at PPARα and PPARγ for analog **3f** (γEC$_{50}$ = 4nM (138%); αEC$_{50}$ = 6 nM (83%), which is a potent dual PPARα/γ agonist.

An X-ray co-crystal structure of **3f** with PPARγ receptor ligand-binding domain (LBD) was determined to 2.25 Å resolution (Fig. 2).[28] Of particular interest to the functional SAR is the H-bonding network observed between ligand carboxylic acid, water and neighboring residues: Ser289 (H3), His323 (H5), His449 (H11) and Tyr473 (H12). In addition to the carboxylate inter-actions, an indirect H-bond is also observed between the oxazole nitrogen, water and Ser342 backbone NH (6–7 loop). The H-bond between Tyr473 on H12 and the carboxylate anion would be expected to be strong and is consistent with the observed superior agonist behavior exhibited by **3f** when compared to its seco analog, the triazole acid **3a**, where the expected trajectory of its carboxylate would not be compatible with a strong H-bond to Tyr473.

Table 4
In vitro PPAR α and γ activities of homologated 3- and 4-triazole analogs

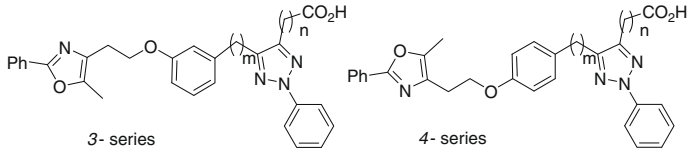

Compound	*m*/*n*	γ IC_{50} (μM)	γ EC_{50} (μM) IA (%)	α IC_{50} (μM)	α EC_{50} (μM) IA (%)	Compound	*m*/*n*	γ IC_{50} (μM)	γ EC_{50} (μM) IA (%)	α IC_{50} (μM)	α EC_{50} (μM) IA (%)
3a	1/0	0.069	3.79 (70%)	0.069	1.90 (30%)	**4a**	1/0	0.712	9.27 (87%)	2.77	6.15 (52%)
3d	0/0	0.67	2.19 (39%)	1.61	4.02 (45%)	**4d**	0/0	1.35	7.33 (23%)	>50	>15
3e	0/1	0.034	0.56 (85%)	0.28	0.39 (72%)	**4e**	0/1	0.517	3.86 (20%)	3.35	4.14 (29%)
3f	1/1	0.005	0.004	0.085	0.006 (83%)	**4f**	1/1	0.007	0.013 (86%)	0.054	0.011 (118%

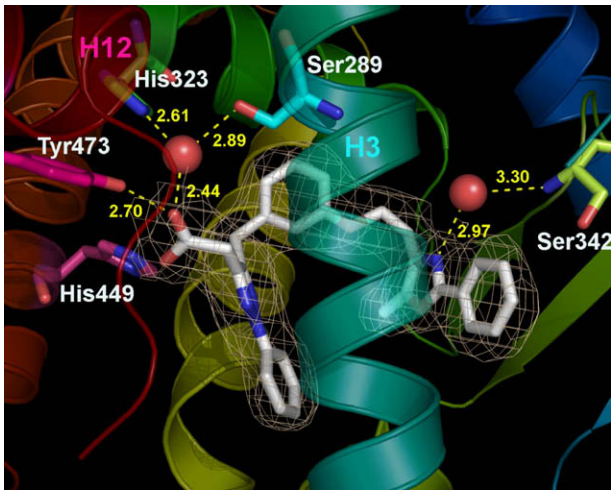

Figure 2. The X-ray structure of **3f** bound to PPARγ LBD is illustrated with ligand electron density shown as a mesh. Residues having significant H-bonding contact with the ligand are highlighted along with two water molecules (red spheres). Distances between heavy atoms are given in Ångstroms.

Table 5
In vivo activity profile of Compound **3f** in *db/db* mice dosed p.o, q.d. for 14 days, overnight fasted

Treatment (10 mg/kg/day for 14 days)	Plasma triglycerides (mg/dL)	Plasma glucose (mg/mL)
Vehicle	156 ± 10	497 ± 32
3f	77 ± 7 (−50%)*	316 ± 34 (−36%)*

* $p < 0.05$.

In the 4-oxyphenyl series, triazole acid analog **4d** ($m = 0$; $n = 0$) showed weak agonist activity only at PPARγ. Addition of a methylene linker to the oxyphenyl ring of **4d** (oxybenzyl analog **4a**) resulted in moderately improved PPARγ (now a full agonist) and PPARα agonist activity versus **4d**. Insertion of a methylene linker between the triazole and carboxylic acid of oxyphenyl analog **4d** ($n = 1$; **4e)** resulted in comparable dual PPARα and PPARγ in vitro activities. Similar to the result from the 1,3-oxyphenyl series, insertion of methylene linkers at both C-4 and C-5 of the triazole ($m = n = 1$; **4f**) also resulted in very substantial improvements in both the PPARγ and PPARα agonist activities (>100-fold) of the oxybenzyl triazole-acetic acid **4f** (now a potent dual PPARα/γ dual agonist) versus the parent oxyphenyl triazole acid **4d**. As shown from the X-ray crystal structure of **3f** bound to PPARγ, the insertion of the two methylene linkers in **3f** and **4f** apparently allows for increased configurational flexibility of the *N*-phenyl azole template, thus enabling these oxybenzyl triazole acetic acid analogs to better form key interactions with key residues such as Tyr473 of PPARγ than the more rigid triazole acids. However, it should be noted that higher binding affinity in the ligand-binding domains (LBDs) of both PPARα and PPARγ does not always necessarily correlate with improved functional agonist activity (e.g., **2a** and **2c** at PPARα).

From these in vitro data, several conclusions can be drawn. First, analogs from the 3-oxybenzyl azole-acid series generally display more equivalent, potent PPARγ and PPARα agonist activity than their 4-oxybenzyl azole-acid counterparts. Second, among the various azole-acid series, analogs with an N^2-phenyl substituent (vs N^1 and N^3) have demonstrated the most potent PPARγ and/or PPARα agonist activities in vitro. Finally, within the triazole acid series, the installation of a methylene linker ($m = 1$, $n = 1$) on either the C-4 or C-5 position of the triazole is preferred for optimal PPARγ and PPARα functional activity. The most potent compound among these triazoles is **3f,** which has increased potency at PPARγ (>10-fold) and at PPARα (>200-fold) relative to muraglitazar (PPARγ $EC_{50} = 35$ nM; IA = 107% and PPARα $EC_{50} = 1.41$ μM; IA = 139%) in vitro.

The in vivo anti-diabetic and lipid-lowering activities of **3f** were further characterized in a 14-day study in female *db/db* mice[29]; the data are shown in Table 5. Compound **3f** (administered orally at a 10 mg/kg/day dose) showed excellent efficacy in significantly reducing levels of plasma glucose (−36%) and triglycerides (−50%) in this diabetic animal model.

In summary, the SAR of a series of *N*-phenyl-substituted azole acid analogs was explored. These studies showed that the PPARγ and α activities in this series can be modulated by: (a) varying the oxybenzyl substitution pattern (3-oxybenzyl series vs 4-oxybenzyl series); (b) the presence of a methylene linker at either the C-4 or C-5 position of the triazole, and (c) the regiochemistry of the preferred *N*-phenyl substituent on the azole ring. In particular, analogs **3f** and **4f** exhibit very potent dual PPARα and PPARγ agonist activity in vitro and analog **3f** also showed excellent anti-diabetic and anti-dyslipidemic activity in the diabetic *db/db* mouse model. In conclusion, we have established a novel series of *N*-phenyl-substituted 1,2,3-triazole acid analogs as a new template/chemotype for the design of potent dual PPARα/γ agonists.

Acknowledgment

We thank the BMS Discovery Analytical Sciences Department for analytical support.

References and notes

1. For general reviews on PPARs (a) Gervois, P.; Fruchart, J.-C.; Staels, B. *Nat. Clin. Practice Endocrinol. Metab.* **2007**, *3*, 145; (b) Pershadsingh, H. A. *Treatments Endocrinol.* **2006**, *5*, 89; (c) Cheng, X.-C.; Xu, W.-F. *Drugs of the Future* **2006**, *31*, 875; (d) Cheng, P. T. W.; Mukherjee, R. *Mini Rev. Med. Chem.* **2005**, *5*, 741.

2. (a) Isseman, I.; Green, S. *Nature* **1990**, *347*, 645; (b) Lee, S. S.; Pineau, T.; Drago, J.; Lee, E. L.; Owens, J. W.; Kroetz, D. L.; Fernandez-Salguero, P. M.; Westphal, H.; Gonzalez, F. *Mol. Cell. Biol.* **1995**, *15*, 3012.
3. Staels, B.; Dallongeville, J.; Auwerx, J.; Schoonjans, K.; Leitersdorf, E.; Fruchart, J.-C. *Circulation* **1998**, *98*, 2088.
4. Todd, P. A.; Ward, A. *Drugs* **1988**, *36*, 314.
5. Malinowski, J. M.; Bolesta, S. *Clin. Ther.* **2000**, *22*, 1151.
6. Gillies, P. S.; Dunn, C. J. *Drugs* **2000**, *60*, 333.
7. (a) Devasthale, P. V.; Chen, S.; Jeon, Y.; Qu, F.; Shao, C.; Wang, W.; Zhang, H.; Farrelly, D.; Golla, R.; Grover, G.; Harrity, T.; Ma, Z.; Moore, L.; Ren, J.; Seethala, R.; Cheng, L.; Sleph, P.; Sun, W.; Tieman, A.; Wetterau, J. R.; Doweyko, A.; Chandrasena, G.; Chang, S. Y.; Humphreys, W. G.; Sasseville, V. G.; Biller, S. A.; Ryono, D. E.; Selan, F.; Hariharan, N.; Cheng, P. T. W. *J. Med. Chem.* **2005**, *48*, 2248; (b) Devasthale, P. V.; Chen, S.; Jeon, Y.; Qu, F.; Ryono, D. E.; Wang, W.; Zhang, H.; Cheng, L.; Farrelly, D.; Golla, R.; Grover, G.; Ma, Z.; Moore, L.; Seethala, R.; Sun, W.; Doweyko, A. M.; Chandrasena, G.; Sleph, P.; Hariharan, N.; Cheng, P. T. W. *Bioorg. Med. Chem. Lett.* **2007**, *17*, 2312; (c) Harrity, T.; Farrelly, D.; Tieman, A.; Chu, C.; Kunselman, L.; Gu, L.; Ponticiello, R.; Cap, M.; Qu, F.; Shao, C.; Wang, W.; Zhang, H.; Chen, S.; Devasthale, P.; Jeon, Y.; Seethala, R.; Ren, J.; Zhou, M.; Ryono, D.; Biller, S.; Mookhtiar, K.; Wetterau, J.; Gregg, R.; Cheng, P. T. W.; Hariharan, N. *Diabetes* **2006**, *55*, 240; (d) Tozzo, E.; Ponticiello, R.; Swartz, J.; Farrelly, D.; Zebo, R.; Welzel, G.; Egan, D.; Kunselman, L.; Peters, A.; Gu, L.; French, M.; Devasthale, P.; Janovitz, E.; Staal, A.; Harrity, T.; Belder, R.; Cheng, P. T.; Whaley, J.; Taylor, S.; Hariharan, N. *J. Pharmacol. Exp. Ther.* **2007**, *321*, 107; (e) Harrity, T.; Chandrasena, G.; Chen, S.; Chu, C.; Devasthale, P.; Farrelly, D.; Jeon, Y.; Kunselman, L.; Qu, F.; Ryono, D.; Sasseville, V.; Selan, F.; Shao, C.; Wang, W.; Wetterau, J.; Zhang, H.; Cheng, P. T. W.; Hariharan, N. *Diabetes* **2002**, *51*, 407.
8. Williams, Johnathan M. J. Ed., Preparation of Alkenes, A Practical Approach, Chapter 2, The Wittig reaction and related methods, Lawrence, N. J. Oxford University Press, 1996.
9. Lam, P. Y. S.; Clark, G. C.; Saubern, S.; Adams, J.; Winters, P. M.; Chan, M. T. D.; Combs, A. *Tetrahedron Lett.* **1998**, *39*, 2941.
10. Skorcz, J. A.; Skorcz, J. A.; Suh, J. T.; Judd, C. I.; Finkelstein, M.; Conway, A. C. *J. Med. Chem.* **1966**, *9*, 656.
11. Kim, Y. H.; Choi, J. Y. *Tetrahedron Lett.* **1996**, *37*, 8771.
12. Kato, T.; Chiba, T. *Chem. Pharm. Bull.* **1975**, *20*, 2203.
13. Garanti, L.; Sala, A.; Zecchi, G. *Synthesis* **1975**, 666.
14. Sabitha, G. *Synth. Commun.* **1998**, *28*, 3065.
15. Almansa, C.; Gómez, L. A.; Cavalcanti, F. L.; Arriba, A. F.; García-Rafanell, J.; Forn, J. *J. Med. Chem.* **1997**, *40*, 547.
16. Pak, C. S.; Yang, H. C.; Choi, E. B. *Synthesis* **1992**, *16*, 1213.
17. Hamanaka, E. S.; Guzman-Perez, A.; Ruggeri, R. B.; Wester, R. T.; Mularski, C. J. Patent application WO9943663.
18. Armani, V.; Dell'Erba, C.; Novi, M.; Petrillo, G.; Tavani, C. Tetrahedron. *1997* **1997**, *53*, 1751.
19. Cheng, P. T. W.; Devasthale, P.; Jeon, Y. T.; Chen, S.; Zhang, H. Patent application WO200121602.
20. Padwa, A.; Prein, M. *J. Org. Chem.* **1997**, *62*, 6842.
21. Ohno, M.; Itoh, M.; Ohashi, T.; Eguchi, S. *Synthesis* **1993**, *08*, 793.
22. Midland, M. M.; Tramontano, A.; Cable; John, R. *J. Org. Chem.* **1980**, *45*, 28.
23. Czernecki, S.; Ville, G. J. *Org. Chem.* **1989**, *54*, 610.
24. Earl, A. R.; Townsend, B. L. *Can. J. Chem.* **1980**, *58*, 2550.
25. Bachmann, W. E.; Struve, W. S. *Org. React.* **1942**, *1*, 38.
26. Seethala, R.; Golla, R.; Ma, Z.; Cheng, L.; Zhang, H.; O'Malley, K.; Lippy, J.; Zhang, L.; Hariharan, N.; Cheng, P. T. W. *Anal. Biochem.* **2007**, *363*, 263.
27. In vitro PPAR agonist functional assays were performed by transiently transfecting GAL4-hPPARα-LBD or GAL4-hPPARγ-LBD constructs, respectively, into HEK293 cells stably expressing 5 copies of GAL4RE-Luciferase. Data were normalized for efficacy at 1 mM to known agonists (rosiglitazone for hPPARγ and GW-2331 for hPPARα). Agonist binding results in an increase in luciferase enzyme activity which can be monitored by measuring luminescence upon cell lysing and the addition of luciferin substrate. EC50 values (μM) for PPARα or γ agonist activity were calculated as the concentration of the test ligand (μM) required for the half-maximal fold induction of HEK293 cells. The "intrinsic activity" of a test ligand is defined as its activity at 1 μM (expressed as a percentage) relative to the activity of the primary standards (GW2331 for PPARα and rosiglitazone for PPARγ, respectively, both tested at 1 μM).
28. PDB deposition number is 3BC5.
29. db/db mice, 8–10 weeks old, fed normal chow ad-lib, were orally dosed with compound or vehicle (5% NMP, 20% PEG-400, 20 mM aqueous sodium phosphate buffer, pH 8) once daily for 14 days. Blood samples were drawn from the tail vein on the 7th day after overnight fasting, and plasma analysis was performed on a COBAS automated analyzer. After 14 days, fasted animals were sacrificed. Blood and tissue samples were collected for clinical biochemistry analyses.